



The first pediatric case of glucagon receptor defect due to biallelic mutations in *GCGR* is identified by newborn screening of elevated arginine



Hong Li^{a,b,*,1}, Lihua Zhao^{c,1}, Rani Singh^{a,b}, J. Nina Ham^d, Doris O. Fadoju^d, Lora J.H. Bean^{a,e}, Yan Zhang^f, Yong Xu^f, H. Eric Xu^{c,g,2}, Michael J. Gambello^{a,b,2}

^a Department of Human Genetics, School of Medicine, Emory University, Atlanta, GA, United States

^b Department of Pediatrics, School of Medicine, Emory University, and Children's Healthcare of Atlanta, Atlanta, GA, United States

^c VARI-SIMM Center for Structure and Function of Drug Targets and the CAS Key Laboratory of Receptor Research, Shanghai Institute of Materia Medica, Chinese Academy of Sciences, Shanghai 201203, China

^d Division of Pediatric Endocrinology, Department of Pediatrics, School of Medicine, Emory University, Children's Healthcare of Atlanta, Atlanta, GA, United States

^e EGL Genetic Diagnostics, Tucker, GA, United States

^f Guangzhou Institutes of Biomedicine and Health, Chinese Academy of Sciences, Guangzhou, 510530, China

^g Laboratory of Structural Sciences, Center for Structural Biology and Drug Discovery, Van Andel Research Institute, Grand Rapids, MI, United States

ARTICLE INFO

Keywords:

Glucagon receptor
Newborn screening
GCGR mutation
Hyperaminoacidemia
Mahvash disease
Pancreatic α cell hyperplasia (ACH)
Pancreatic neuroendocrine tumor (PNET)

ABSTRACT

Glucagon receptor (*GCGR*) defect (Mahvash disease) is an autosomal recessive hereditary pancreatic neuroendocrine tumor (PNET) syndrome that has only been reported in adults with pancreatic α cell hyperplasia and PNETs. We describe a 7-year-old girl with persistent hyperaminoacidemia, notable for elevations of glutamine (normal ammonia), alanine (normal lactate), dibasic amino acids (arginine, lysine and ornithine), threonine and serine. She initially was brought to medical attention by an elevated arginine on newborn screening (NBS) and treated for presumed arginase deficiency with a low protein diet, essential amino acids formula and an ammonia scavenger drug. This treatment normalized plasma amino acids. She had intermittent emesis and anorexia, but was intellectually normal. Arginase enzyme assay and *ARG1* sequencing and deletion/duplication analysis were normal. Treatments were stopped, but similar pattern of hyperaminoacidemia recurred. She also had hypercholesterolemia type IIa, with only elevated LDL cholesterol, despite an extremely lean body habitus. Exome sequencing was initially non-diagnostic. Through a literature search, we recognized the pattern of hyperaminoacidemia was strikingly similar to that reported in the *Gcgr*^{-/-} knockout mice. Subsequently the patient was found to have an extremely elevated plasma glucagon and a novel, homozygous c.958_960del (p.Phe320del) variant in *GCGR*. Functional studies confirmed the pathogenicity of this variant. This case expands the clinical phenotype of *GCGR* defect in children and emphasizes the clinical utility of plasma amino acids in screening, diagnosis and monitoring glucagon signaling interruption. Early identification of a *GCGR* defect may provide an opportunity for potential beneficial treatment for an adult onset tumor predisposition disease.

1. Introduction

The glucagon receptor (*GCGR*) is a G-protein-coupled receptor expressed mainly in the liver and kidney. Upon glucagon binding, it activates the stimulatory G protein (Gs) and increases cAMP level, subsequently transducing glucagon signaling involved in glucose, amino acids and lipid metabolism [1]. Mahvash disease is the only reported

human phenotype associated with glucagon receptor defect. It is an autosomal recessive hereditary pancreatic neuroendocrine tumor (PNET) syndrome caused by biallelic inactivating mutations in *GCGR* gene [2]. Since first reported in 2008, 11 cases have been described [3,4]. All are adult patients with variable age at diagnosis (25–74 years old); no pediatric cases have been reported, nor is there much known about the pediatric medical histories of the affected adults. The typical

* Corresponding author at: Division of Medical Genetics, Department of Human Genetics, School of Medicine, Emory University, 1365 Clifton Rd. NE, Building B, Suite 2200, Atlanta, GA, 30322, United States.

E-mail address: Hong.Li@emory.edu (H. Li).

¹ Both authors contributed equally to this work

² Co-senior authors.

<https://doi.org/10.1016/j.ymgmr.2018.09.006>

Received 17 July 2018; Received in revised form 18 September 2018; Accepted 18 September 2018

2214-4269/© 2018 The Authors. Published by Elsevier Inc. This is an open access article under the CC BY-NC-ND license (<http://creativecommons.org/licenses/by-nc-nd/4.0/>).

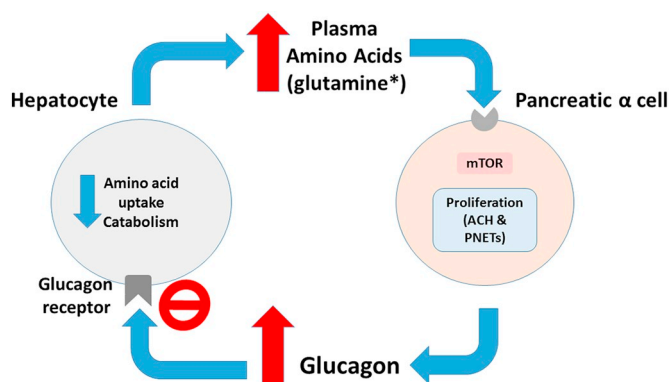


Fig. 1. The hepatic α cell axis feedback loop underlies the pathogenesis of glucagon receptor defect in $Gcgr^{-/-}$ mice. Interrupted glucagon signaling secondary to glucagon receptor defect in hepatocytes leads to decreased hepatic amino acids uptake and catabolism, and increased plasma amino acids. The hyperaminoacidemia, especially glutamine (*), activates pancreatic islet α cell proliferation partially through mTOR dependent mechanisms. This activation results in pancreatic α cell hyperplasia (ACH) with or without pancreatic neuroendocrine tumors (PNETs), and increases glucagon production (hyperglucagonemia). mTOR: mechanistic target of rapamycin. Adapted from [5,6].

presentation is non-specific abdominal pain and subsequent abdomen imaging study identifies pancreatomegaly with or without clear masses. The pathological findings are characterized by diffuse pancreatic α cell hyperplasia (ACH) with or without PNETs. Although patients have extreme hyperglucagonemia, there is no evidence of glucagonoma syndrome, such as skin rash, stomatitis, hyperglycemia or weight loss, because of the dysfunctional GCGR.

In the murine $Gcgr^{-/-}$ model, the complete block in glucagon signaling reduces hepatic uptake and catabolism of amino acids by altering hepatic gene expression of amino acid transporters and catabolic enzymes. As a consequence, circulating plasma amino acids are elevated [5,6]. Hyperaminoacidemia, especially elevated L-glutamine, stimulates mTOR signaling leading to pancreatic ACH and increased glucagon production, thus revealing a hepatic α cell axis as the basis of strong negative feedback mechanism in $Gcgr^{-/-}$ mice [5,6], which is outlined in Fig. 1. Hyperaminoacidemia was also reported in a patient with Mahvash disease [7], however, it is unknown if hyperaminoacidemia is a feature of all cases of GCGR defect, even pre-symptomatically.

Here, we describe the first pediatric case of glucagon receptor defect due to biallelic mutations in the *GCGR*, uniquely identified by positive newborn screening (NBS) for elevated arginine. Although expanded NBS has allowed the identification of many inborn errors of metabolism, GCGR defect associated with hyperargininemia or hyperaminoacidemia has never been considered or reported though NBS [8]. The similar pattern of plasma amino acids in the $Gcgr^{-/-}$ mouse and our case, previously unrecognized, may represent an early opportunity to detect asymptomatic Mahvash patients.

2. Patients and methods

2.1. Subject

The patient's information was all collected clinically in order to make the diagnosis and guide the management and surveillance. Informed consent was obtained from parents for the use of this information. Clinical exome analysis was performed (EGL Genetic Diagnostics, Tucker GA) using the V5Plus exome capture method (Agilent, Santa Clara, CA), NextGene alignment (SoftGenetics, State College, CA) and analyzed using an in-house bioinformatics pipeline. The NM_000160.3:c.958_960del (p.Phe320del) variant was confirmed

by Sanger sequencing in the proband and both parents. Functional studies proved its pathogenicity.

2.2. Elective fasting hypoglycemia test

To investigate our patient's fasting tolerance, a hospital-based controlled fasting study was done clinically.

2.3. Functional studies of the novel variant in *GCGR*

2.3.1. Plasmid construction

Human glucagon receptor (GCGR) without the predicted signal peptide coding region was synthesized by Genewiz (Beijing, China). The encoded fragments were digested with *Bam*HI and *Not*I restriction endonucleases, then they were inserted into a modified pcDNA6 expression vector which encodes a fusion protein consisting of an N-terminal human IgG leader (MGWSCIIIFLVATATGVHSE) for targeting the protein into the cell membrane. It also has a FLAG tag (DYKDDDD) at the C-terminus for detection by immunoblotting. Fused GCGR represents self-activation construct which tethers the glucagon peptide hormones (GCG) to the full-length receptor with a FLAG-GSA5 linker and constitutively activates receptor signaling; full-length (FL) GCGR needs glucagon binding to activate (Fig. 4A). For the GCGR localization assays, we added sfGFP at the N-terminal of the constructs above [9]. All of these constructs contain the same IgG leader, as described above.

2.3.2. cAMP assay

Wild-type and mutant (p.Phe320del) GCGR were transiently expressed in HEK293 suspension cells. Site-directed mutagenesis experiments were carried out using the QuikChange method (Agilent) and all plasmid constructs were confirmed by DNA sequencing (Genewiz). Cells were transfected using Lipofectamine reagent (Life Technologies) with 200 ng CRE-driven fly luciferase reporter, 10 ng TK promoter driven renilla luciferase and 50 ng cDNA of GCGR. TK was used as an internal transfection controls. After three hours transfection, the cells were treated with 1 μ M doxycycline for 24 h, then glucagon with concentration of 0 nM and 500 nM were added to cells for 4 h incubation. We assessed GCGR activity by measuring the cAMP signal, which is the activity of cAMP-responsive CRE-driven fly luciferase reporter relative to renilla luciferase activity (RLU) from different constructions of GCGR. This activity was measured by the EnVision plate reader (PerkinElmer), according to the manufacturer's instructions for the Dual-luciferase reporter assay system from Promega [9]. GCG dose response curves of FL and fused human GCGR WT and p.phe320del mutant were conducted.

2.3.3. GCGR localization assay

Confocal microscopy imaging was performed to monitor the location of GCGR in live cells. The HEK293 suspension cells (1×10^5) were seeded in a 35 mm glass bottom dish and transfected with a modified pcDNA6 expression vector, pcDNA6-sfGFP-GCGR and pcDNA6-sfGFP-GCG(1-29)-FLAG-5GSA-GCGR, including Wild-type GCGR and p.Phe320del. We confirmed the expression and location of GCGR by confocal microscopy imaging. (Cell Observer SD, Zeiss, Germany).

2.3.4. Western blot analysis

The HEK293 suspension cells were harvested by centrifugation, then their pellets solubilized in cell lysis reagent (CellLyticTM M, Sigma) supplemented with 1 mM PMSF and centrifuged at $16,000 \times g$ for 30 min. The supernatants were subjected to SDS-PAGE and transferred to PVDF membranes, and the membranes were blocked with 5% milk in TBST (20 mM Tris-HCl pH 8.0, 150 mM NaCl and 0.05% Tween-20), then incubated with anti-FLAG M2 antibodies from mouse (Sigma) or monoclonal anti- β -actin antibody from mouse clone AC-15 (Sigma), followed by anti-mouse HRP antibodies in 5% milk in TBST. The images were collected using ChemiDocTM XRS+ imager (BIO-RAD) [9].

2.3.5. Molecular modeling

The GCGR p.Phe320del model was built with the Prime module (Schrödinger, LLC) using the structure of wild-type GCGR as the template (PDB Code: 5yqz.pdb) [10]. The homology model was subjected to energy minimization while freezing the residues from the beginning to residue 319.

3. Results

3.1. Case presentation

The patient was a 7-year-old fraternal twin female, born at 35 weeks gestation, to Indian parents who were first cousins once removed. Birth measurements were: weight 2296 kg (25%ile) and length 46 cm (25%ile). Her first NBS at day of life 1 (DOL1) was positive for elevated TSH 35.7uU/mL (cut off < 25), and repeat NBS at DOL9 was normal. A third NBS at DOL30, based on state prematurity protocol, revealed an elevated plasma arginine of 186.1 μmol/L (cut off < 105). Given two previous normal NBS for arginine level, another NBS at 38 days was collected and arginine remained elevated at 135 μmol/L. Confirmatory plasma amino acid (PAA) analysis at 2 months old showed multiple amino acids elevations, especially glutamine 1647 μmol/L (246–984), alanine 832 μmol/L (124–573) and arginine 349 μmol/L (20–148) (Table 1), but normal ammonia level 15.8 μmol/L (15–47). She received a presumptive diagnosis of arginase deficiency and treated with low protein diet supplemented with essential amino acids formula Cyclinex-1 (Abbott Nutrition, USA) and an ammonia scavenger drug sodium phenylbutyrate. In spite of this diagnosis, her ammonia levels were always normal, ranging from 8 to 37 μmol/L. Urine orotic acid, urine amino acids, serum lactic acid level, and serum transaminases were all normal. Plasma amino acids during treatment essentially normalized the majority of the time, including arginine levels. Ornithine levels were normal or even above normal instead of the anticipated low levels seen in arginase deficiency. Both red blood cell arginase enzyme activity and *ARG1* sequencing and deletion/duplication analysis were normal. Biochemical and genetic studies were not consistent with arginase deficiency.

Clinically the patient had a history of anorexia and intermittent emesis. These symptoms prompted G-tube placement. Her neurologic exam was completely normal with no signs of intellectual disability or spasticity, commonly seen in patients with arginase deficiency. An alternative diagnosis was investigated at 4 years of age.

We took a stepwise approach to wean her treatments. First we stopped her sodium phenylbutyrate but maintained a low protein diet supplemented with Cyclinex-2 (Abbott Nutrition, USA). Her plasma amino acids remained normal suggesting that the ammonia scavenger was not essential. Second, we discontinued the Cyclinex-2 formula and started a diet with age and gender-appropriate dietary reference intakes (DRI) for protein. Surprisingly, the similar pattern of hyperaminoacidemia recurred, consisting of predominantly glutamine, alanine, lysine, arginine, ornithine, threonine and serine. Anorexia with intermittent emesis persisted. Her growth curve had been almost flat from 4 years of age to 7 years of age despite sufficient caloric support. At 7 years of age her growth parameters were as follows: weight 15.25 kg (z-score: -3.96), height 113.7 cm (z-score:-2.32), head circumference 49.5 cm (z-score:-0.38), BMI 11.8 (z-score:-3.79). (Fig. 2).

The elevated plasma levels of glutamine and arginine raised a concern that there might be CNS toxicity, therefore she had a thorough neurologic evaluation. Remarkably, her cerebrospinal fluid (CSF) amino acids and brain MRI/MRS were all normal in spite of plasma hyperaminoacidemia. She also had hypercholesterolemia, with an elevated low density lipoprotein cholesterol (LDL-C) level, normal triglyceride and high density lipoprotein cholesterol (HDL-C) level, despite an extremely lean body habitus. Family fasting lipid studies revealed the mother had normal lipid profile and father had mild hyperlipidemia with both LDL-C and triglyceride elevations but low HDL-C. (Table 2).

Exome sequencing with deletion and duplication analysis was initially reported as normal.

Through a PubMed search via “hyperaminoacidemia”, we recognized that her unique pattern of hyperaminoacidemia looked almost exactly like that reported in the glucagon receptor knockout (*Gcgr*^{-/-}) mice [11]. Although exome analysis performed at four years of age was initially non-diagnostic, reanalysis specifically for the *GCGR* gene [MIM: 138033] identified a homozygous c.958_960del (p.Phe320del) variant, which had no previous disease association and is present as only a single allele in the Genome Aggregation Database (gnomAD; <http://gnomad.broadinstitute.org>). Both parents were heterozygous for the variant.

Her fasting plasma glucagon level was 27,000 pg/dL (Reference value < 280) but no signs or symptoms of glucagonoma syndrome, further supporting the diagnosis of *GCGR* defect. Abdominal MRI showed normal pancreas size and structure at 7 years of age.

3.2. Characterization of plasma amino acid profile

Elevation of multiple amino acids was demonstrated on PAA analysis collected 4–5 h postprandially. Predominantly, glutamine, alanine, dibasic amino acids (lysine, arginine, and ornithine), threonine, and serine were persistently elevated. Essential amino acids, such as phenylalanine and branched-chain amino acids, were less affected and essentially normal. The profile was highly correlated with the amount of natural protein (NP) intake and the timing of sample collection. During the first 4 years of life, a very low NP diet supplemented with Cyclinex-1 or -2 (essential AA formula) essentially normalized PAA. After her natural protein intake was liberalized at 7 years of age, her PAA profile showed more generalized elevations, and glutamine level was not fully normalized despite an ammonia scavenger glycerol phenylbutyrate. After overnight (data not shown) and prolonged fasting, the PAA was close to normal. (Table 1).

3.3. Elective fasting hypoglycemia test result

The patient demonstrated fasting tolerance of 21.5 h until glucose dropped < 50 mg/dL. She had appropriate ketone production, normal lactate level, and appropriate counter-regulatory hormone levels, including cortisol and growth hormone, at the time of hypoglycemia. Prolonged fasting plasma amino acids (21.5 h fasting) were essentially normal. Glucagon stimulation test was completely unresponsive up to 30 mins after glucagon administration, as expected. Glucose rapidly increased after drinking juice. (Fig.3).

3.4. Functional studies of the novel variant

3.4.1. cAMP assay

To examine the function of mutant *GCGR* protein (p.Phe320del), p.Phe320 deletion was created in the full-length receptor *GCGR* cDNA and a fusion receptor was constructed, in which glucagon (amino acids 1–29) and the *GCGR* are separated by a FLAG-GSA5 linker as shown in Fig.4A. The wild-type *GCGR* and p.Phe320del-expressing constructs were transiently expressed in HEK293 suspension cells. We monitor *GCGR* signaling in the presence and absence of 500 nM glucagon by measuring the activation of a cAMP-responsive CRE-luciferase reporter. The physiological GCG concentration in blood is ~25 pM [12,13], as shown in Fig.4B. Both p.Phe320del in full-length receptor *GCGR* and a fusion receptor generate no cAMP signal compared to wildtype. This indicates complete loss of function mediated by cAMP signaling. GCG dose response curves were then determined with WT and p.Phe320del mutant FL and fused human *GCGR* constructs. It showed the EC50 concentration for GCG to activate the WT FL human *GCGR* is only 2.041 nM (log [2.041] = 0.3). For both p.Phe320del mutant FL and fused *GCGR* constructs, there is very low activation up to 1 × 10⁵ nM (log [1 × 10⁵] = 5) GCG (Fig.4C).

Table 1
Characterization of plasma amino acids

Age	2m	4y 3m	4y 5m	4y 7m	5y 4m	7y 9m	7y 11m	
Diet protein	6.7g NP	16g NP + 4.5g Cyclinex-2	11g NP + 4g Cyclinex-2	19.5g NP	30g NP	41g NP	41g NP	
TP (g/kg/d)	2.1	1.6 (NP 1.2)	1.2 (NP 0.8)	1.5	2.3	-	2.75	
Ammonia scavenger	-	Buphenyl® 120 mg/kg/d	-	-	-	Ravicti® 9.5 ml/m ² /d	-	
Post-prandial collection time (hours)	3	4	4	4.5	4	5	4.5	21.5
Glutamine	1647 (246-984)*	765 (254-823)**	778	1094	1313	1022	901	694
Alanine	832 (124-573)	493 (152-547)	428	580	1117	931	783	477
Arginine	349 (20-148)	126 (10-140)	132	232	240	326	298	150
Lysine	544 (43-243)	292 (48-284)	318	399	450	728	499	261
Ornithine	238 (190-173)	63 (10-163)	110	213	153	224	187	203
Threonine	558 (50-248)	161 (35-226)	214	294	319	452	347	184
Serine	279 (90-209)	126 (69-187)	113	209	241	291	204	145
Glycine	366 (125-497)	195 (127-341)	232	309	383	324	312	228
Tyrosine	123 (24-129)	65 (24-115)	83	112	112	179	129	71
Methionine	58 (17-49)	16 (7-47)	23	28	39	73	41	22
Citrulline	31 (6-52)	25 (1-46)	34	47	59	33	49	33
Leucine	148 (29-151)	80 (49-216)	108	125	154	239	152	179
Valine	245 (67-299)	186 (74-321)	222	251	307	376	283	299
Isoleucine	84 (20-96)	40 (22-107)	56	64	84	142	86	110
Phenylalanine	53 (37-86)	33 (26-91)	43	56	64	95	65	50
Proline	314 (88-417)	106 (59-369)	110	267	460	549	368	208

Notes: NP natural protein. TP: total protein. *Reference range for < 2y, amino acid unit: $\mu\text{mol/L}$. ** Reference range for > 2y. Buphenyl®: sodium phenylbutyrate. Ravicti®: glycerol phenylbutyrate. Elevated amino acids level are in bold, predominantly elevated amino acids are in bolded box.

3.4.2. GCGR localization assay

The fluorescent GCGR signal was observed mainly on the surface of cells after transfection with a modified pcDNA6 expression vector with sfGFP-GCGR, sfGFP- p.Phe320del, sfGFP- GCG-GCGR fusion protein, and sfGFP- GCG-GCGR fusion protein of p.Phe320del respectively. Both wild-type GCGR and p.Phe320del expression detected on cell-surface in HEK293 suspension cells. As shown in Fig. 4D, these data suggest that the p.Phe320del does not affect normal intracellular trafficking to the cell membrane.

3.4.3. Western blot analysis

The expression of GCGR in HEK293 suspension cells was further analyzed by Western blot with anti-FLAG antibody. As shown in Fig. 4E, the band of wild-type GCGR protein was clearly visualized in full-length receptor and the fusion protein from the cell lysates, but not seen is the band of p.Phe320del GCGR protein from the cell lysates, most of the p.Phe320del protein was in the precipitate, and considerably degraded. These results suggest that p.Phe320del protein may be more unstable than wild-type GCGR protein.

3.4.4. GCGR computer modeling

Computer modeling demonstrated a rotation of the transmembrane domain 5 (TMD5) helix that may cause a conformational change leading to defective GCGR signaling. The comparison of the sequence and structure of wild-type GCGR and p.Phe320del GCGR shows that the helix part rotates with one residue and may cause conformational change. This conformational change in TMD5 may result in altered G protein binding and therefore signaling (Fig. 4F.).

4. Discussion

All previously reported cases of glucagon receptor defect (Mahvash disease) have been diagnosed in symptomatic adults with the finding of pancreatic ACH with or without PNETHs. To our knowledge, this is the first pediatric case of GCGR defect presymptomatically identified by an elevated arginine level on NBS. The similarity of her persistent hyperaminoacidemia to that of the *Gcgr*^{-/-} mouse model of Mahvash disease lead to the ultimate diagnosis, confirmed by extreme hyperglucagonemia and biallelic inactivating *GCGR* mutations. Functional studies of the novel homozygous c.958_960del (p.Phe320del) variant in *GCGR* demonstrated nearly complete inhibition of glucagon signaling. This case adds a pediatric phenotype to the clinical spectrum of human GCGR defect.

The hyperaminoacidemia is characterized by elevations of glutamine, alanine, dibasic amino acids (arginine, lysine and ornithine), threonine, and serine after 4–5 h fasting. Essential amino acids, such as phenylalanine and branch-chain amino acids (BCAAs) are usually not elevated unless protein intake is quite high (Table 1). Notably, this pattern can be affected not only by protein intake, but also the timing of specimen collection. Hyperaminoacidemia can be essentially normalized after overnight fasting. Therefore, a normal amino acid profile in the setting of low natural protein intake or prolong fasting does not rule out GCGR defect. Larger et al. reported hyperaminoacidemia, particularly the glucogenic amino acids, in a 54-year old patient with symptomatic GCGR defect. Like our patient, alanine was elevated at 978 $\mu\text{mol/L}$ (normal range, 250–400 $\mu\text{mol/L}$), but a complete amino acid profile was not provided. Here, we report a detailed characterization of the plasma amino acid pattern from our patient. We propose that this unique amino acid profile can be used to identify other patients with GCGR defect. The characteristic profile will aid biochemical

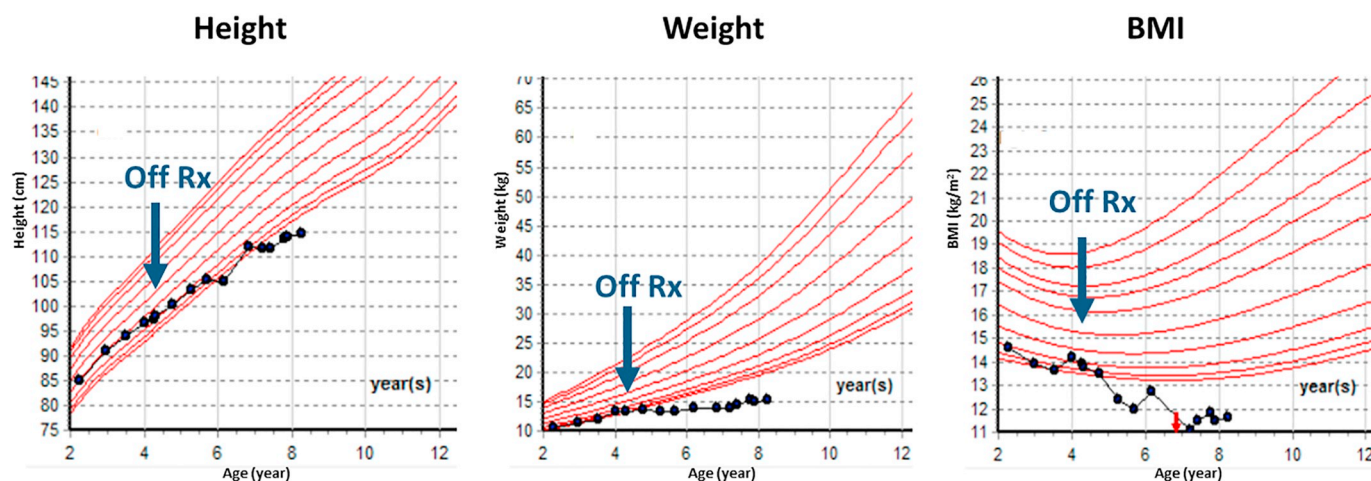


Fig. 2. Height, weight and BMI growth curves. After discontinuation of treatment (Rx–low protein diet supplemented with Cyclinex-2 and ammonia scavenger), marked by big blue arrow, there has been almost no weight increase, accompanied by decreased growth velocity and BMI. Small red arrow indicates BMI 11. (For interpretation of the references to colour in this figure legend, the reader is referred to the web version of this article.)

Table 2

Fasting lipid profile.

Lipid profile	Total-cholesterol mg/dL	HDL-cholesterol mg/dL	LDL-cholesterol mg/dL	Triglycerides mg/dL
Patient	278 (< 170)	72 (> 45)	174 (<110)	45 (< 75)
Father	255 (100–199)	25 (> 39)	189 (0–99)	171 (0–149)
Mother	190 (100–199)	57 (> 39)	114 (0–99)	96 (0–149)

genetics laboratories to consider glucagon signaling abnormalities in the differential diagnosis and ensure appropriate follow-up. Importantly, more patients might be identified by the NBS for elevated arginine level, like our patient, thereby further expanding the spectrum of GCGR defect. Currently, pharmacologic inhibition of the glucagon receptor is a potential treatment of diabetes mellitus. It is unclear if this inhibition could cause a similar hyperaminoacidemia characteristic of GCGR defect. It may be prudent to assess plasma amino acid profiles as part of the clinical trials for these drugs. One long-term consequence could be unintentionally activating the alpha cell axis thereby stimulating ACH and tumor development.

The elective controlled fasting study in our patient provides further metabolic profiling in patients with GCGR defect. Despite her lean body mass with low weight, at the age of 7 years old she demonstrated a good tolerance for fasting with hypoglycemia < 50 mg/dL occurring at 21.5 h fasting (Fig. 3). During fasting, ketone production, lactic acid level, insulin, and counter-regulatory hormones levels, such as growth hormone and cortisol, were all appropriate. Not surprisingly, she had no response to synthetic exogenous glucagon injection. The normal lactate at the time of hypoglycemia suggested unimpaired gluconeogenesis.

Her gastrointestinal (GI) symptoms have been puzzling. Control of appetite and food intake is complex and the exact mechanisms of GI presentation in our patient is unknown. Her lean body mass, failure to thrive, anorexia, and intermittent vomiting are symptoms not reported in previously diagnosed adult patients. However, the reported cases of Mahvash disease focused on pancreatic ACH cell hyperplasia and PNETs, and detailed past medical histories in childhood were not available. Although we certainly can't completely rule out other defects, in addition to the GCGR defect, which lead to the observed GI effects in our patient, the variability of clinical presentation may also be determined by the various degree of GCGR inhibition due to different genotype.

We reviewed the spectrum of GCGR mutations in adult cases as well as our case of GCGR defect and demonstrated it in Fig.5 [2,4,7,14]. Notably, all adult patients, except one, carry mutations that lead to a complete loss of GCGR function. The nonsense, frameshift or splice acceptor site mutations (purple and green arrows, Fig.5) introduce premature stop codons and produce no protein or truncated protein. Two missense mutations (yellow arrows, Fig.5), c.256C > T (p.P86S) and c.187G > A (p.D63N), affect GCGR protein intracellular trafficking and abnormal localization to the endoplasmic reticulum rather than the cell membrane. So all these adult GCGR mutations cause complete loss of GCGR function. The patient reported by Sipos et al. carries two homozygous (blue arrows, Fig. 5) variants in GCGR, c.674G > A (p.R225H) and c.1102G > A (p.V368M) [14]. The significance of either variant is uncertain. First, the glucagon level in this patient is unknown and the diagnosis of Mahvash disease is uncertain. Secondly, these two missense variants are predicted to be damaging by *in silico* analysis. No functional studies were conducted. Lastly, individuals homozygous for either variant are seen in gnomAD. There are 41 GCGR c.674G > A (p.R225H) alleles in gnomAD with 2

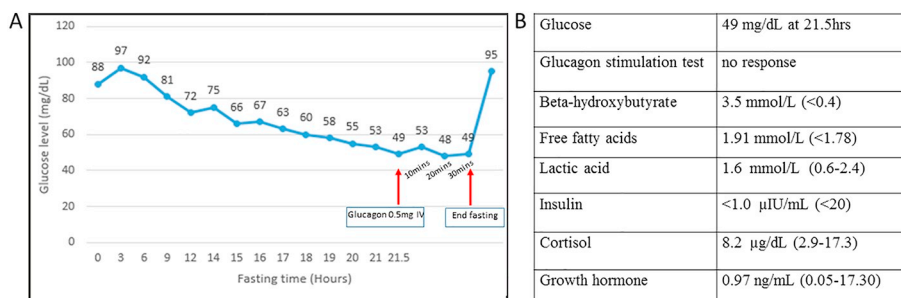


Fig. 3. Controlled fasting data. A. The patient demonstrated 21.5 h fasting tolerance until glucose < 50 mg/dL.; glucose level was unresponsive to glucagon stimulation test; B. Appropriate ketone production, lactate and hormone levels in response to fasting glucose level (at 21.5 h.).

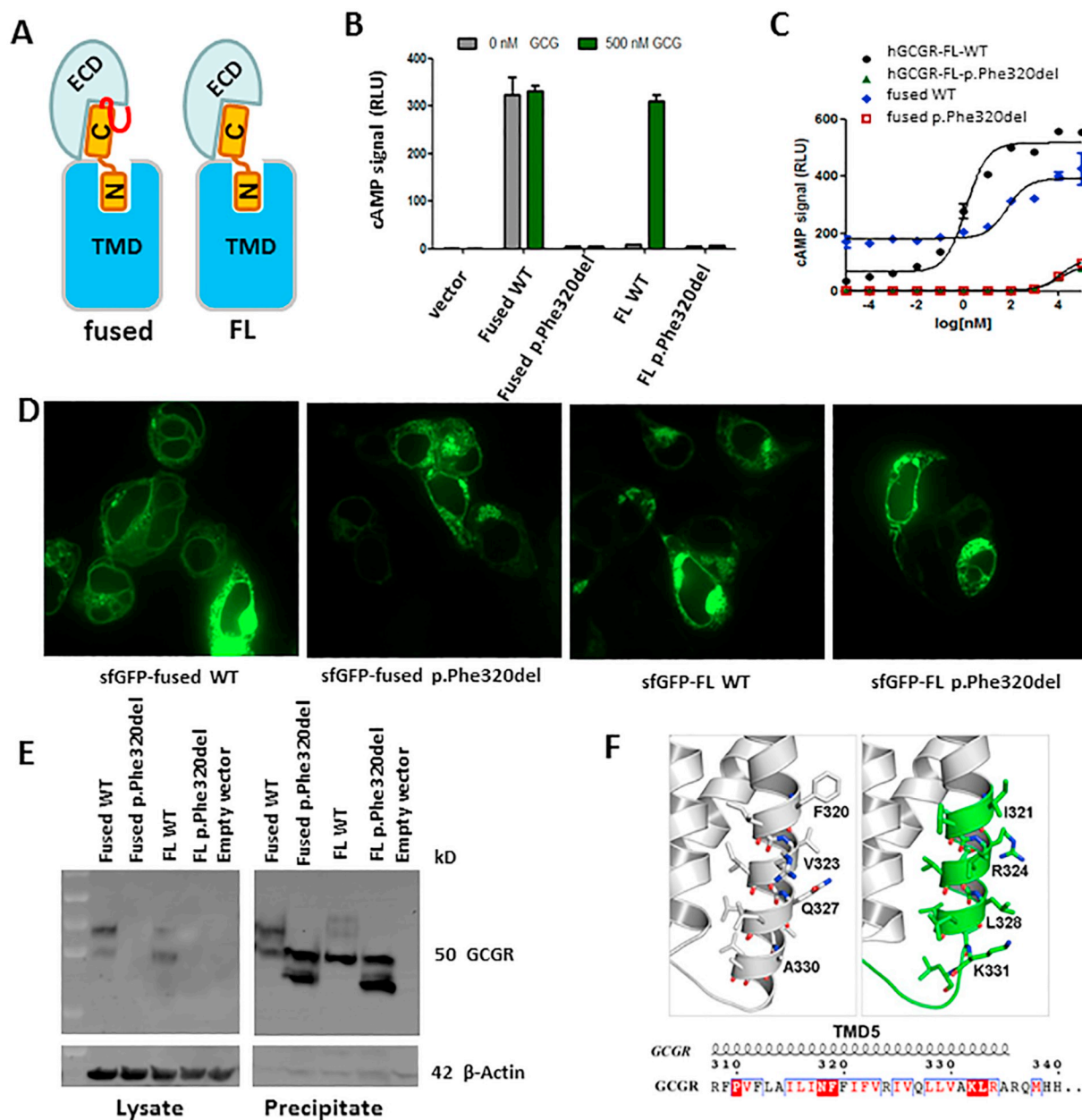


Fig. 4. Functional studies of GCGR p.Phe320del. **A.** Schematic representation of constructs. Fused: fusion between glucagon peptide hormone (GCG, red curve) to full length glucagon receptor (GCGR), serves as a self-activated GCGR construction. FL: full length glucagon receptor, ECD: extracellular domain, TMD: transmembrane domain, N: N terminus, C: c-terminus. **B.** Activation of GCGR measured by cAMP signals, which are relative luciferase (RLU) activities of the different constructs in the absence (0 nM) or presence (500 nM) of exogenous glucagon peptide hormone (GCG). Note the virtual absence of cAMP signal of the mutant GCGR p.Phe320del. **C.** GCG dose response curves of WT and p.Phe320del mutant FL human GCGR, and WT and p.Phe320del mutant fused human GCGR constructs, the EC50 value for GCG is 2.041 nM ($\log [2.041] = 0.3$), for both FL and fused p.Phe320del, there is very low activation up to 1×10^5 nM ($\log [1 \times 10^5] = 5$) GCG. $n = 3$, error bars = S.D. **D.** Localization of sfGFP-GCGR wild type (WT) and GCGR mutant p.Phe320del in HEK293 suspension cells. WT and p.Phe320del GCGR are both expressed on the cell surface. **E.** Expression levels of GCGR WT and GCGR p.Phe320del protein from lysate and precipitate, determined by immunoblotting using anti-FLAG antibody. GCGR p.Phe320del protein was only detected in precipitate with a considerable degradation, which may suggest its instability. **F.** Computer modeling of wild type (F320, left) and p.Phe320 deletion (right) GCGR and the transmembrane domain 5 (TMD5) regions are shown. Residues with conformational change were labeled and shown as sticks. (For interpretation of the references to colour in this figure legend, the reader is referred to the web version of this article.)

homozygotes (minor allele frequency 0.175 in South Asians) and 10 alleles of c.1102G > A (p.V368M) in gnomAD with 1 homozygote (highest minor allele frequency 0.026). Based on the above information, the clinical significance of both variants is unknown underscoring the importance of functional studies as we have done. The novel variant identified in our patient leads to a single amino acid deletion that does not affect GCGR production nor cell membrane localization (see Fig. 4). The conformational change in TMD5 predicted by computer modeling may result in intracellular altered G protein binding and signaling.

Although we demonstrated the loss of function mediated by attenuated cAMP signaling but this does not rule out other cAMP-independent intracellular pathways are still able to be activated through this mutant GCGR, especially exposed to supraphysiological glucagon level.

Interestingly, an observed side effect of IV administration of glucagon in normal individuals during the glucagon stimulation test is nausea and vomiting. Presumably the intact GCGR modulates an intracellular signal in response to a supraphysiologic dose of glucagon. In our patient, the GCGR is localized to the membrane. We hypothesize

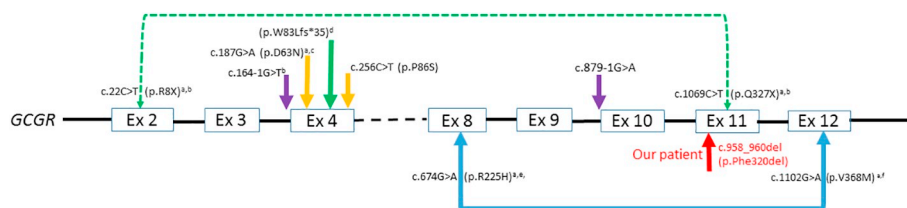


Fig. 5. Human GCGR mutation spectrum.

All solid arrow indicates homozygous variant in each reported case. The two linked dot arrows indicate compound heterozygous variants in the same patient. Yellow arrow: the variant affects GCGR protein intracellular trafficking and abnormal GCGR localization to endoplasmic reticulum rather than the cell membrane; Green arrow: the variant is either non-sense or frameshift mutation predicted to produce no

protein or truncated protein; Purple arrow: the splice acceptor site variant leads to altered splicing and introduces a premature stop codon; Blue arrow: The two homozygous variants were identified in the same patient. Both variants are predicted to be damaging but no functional studies were done. Homozygotes for either allele are found in gnomAD (see below); Red arrow: variant identified in our case that does not affect GCGR protein production nor membrane localization. The nomenclature is based on reference sequence NM_000160.4. ^a. nucleotide change (c. nomenclature) was not provided in published report and, therefore, has been inferred from population data; ^b. 1 allele in gnomAD; ^c. 4 alleles in gnomAD; ^d. DNA change cannot be inferred from published paper; ^e. 41 alleles in gnomAD with 2 homozygotes (minor allele frequency 0.175 in South Asians); ^f. 10 alleles in gnomAD with 1 homozygote (highest minor allele frequency 0.026).

that the pathway leading to GI symptoms remains intact in spite of the p.Phe320del. In all other patients there is no GCGR localized to the membrane, so consequently no GI symptoms. The molecular details of such a mechanism will be the subject of future research.

Notably, our patient also had hypercholesterolemia. Her lipid profile of high LDL-C, normal HDL-C and triglyceride is consistent with type IIa hypercholesterolemia. Her exome analysis did not reveal pathogenic variants in any of the known genes associated with hypercholesterolemia, including *LDLR* [MIM: 606945], *APOB* [MIM: 107730], and *PCSK9* [MIM: 607786]. Both *Gcgr*^{-/-} and liver specific siRNA-mediated *Gcgr* inhibition in mice showed elevations of cholesterol, especially LDL-C. Similar LDL-C elevations were observed in patients with type 2 diabetes who were treated with a GCGR antagonist [15–17]. The elevated LDL-C in our patient is likely secondary to the GCGR defect, but there may also be an aspect of familial hyperlipidemia as shown in Table 2.

5. Conclusion

This novel pediatric case of GCGR defect, identified by abnormal NBS, expands the clinical spectrum beyond adult pancreatic ACH and PNETs. The recognizable pattern of hyperaminoacidemia sheds light on early screening and diagnosis of conditions associated with glucagon signaling interruption. Though glutamine is the main trigger for pancreatic ACH in the mouse, its role in human disease is unclear. Upon retrospective review of our patient's plasma amino acid profiles, the majority of her profiles were normalized and her growth velocity was better while she was treated with a low protein diet supplemented with an essential amino acid formula. The role of dietary management in patients with GCGR defect requires further investigation.

Financial disclosure

The authors have no conflicts of interest to disclose.

Conflict of interest

The authors have no conflicts of interest to disclose.

This manuscript has not been published. It will not be submitted elsewhere while under consideration and, should it be published in *Molecular Genetics and Metabolism*, it will not be published elsewhere – either in similar form or verbatim – without permission of the editors.

Acknowledgements

We thank Run Yu, MD, PhD (Division of Endocrinology, Diabetes, and Metabolism, UCLA David Geffen School of Medicine, Los Angeles, California) for his expert input on this rare condition.

Functional studies were supported by grants the Youth Innovation Promotion Association and Natural Science Foundation of Shanghai, China (18ZR1447800 to L.H.Z.), National Institutes of Health, United

State (DK071662 to H.E.X.). It was also partially supported by the Fudan-SIMM Joint Research Fund, China (FU-SIMM-20174003) and the Support of SA-SIBS Scholarship Program.

References

- [1] K.M. Habegger, K.M. Heppner, N. Geary, T.J. Bartness, R. Dimarchi, M.H. Tschop, The metabolic actions of glucagon revisited, *Nat. Rev. Endocrinol.* 6 (12) (2010) 689–697.
- [2] C. Zhou, D. Dhall, N.N. Nissen, C.R. Chen, R. Yu, Homozygous P86S mutation of the human glucagon receptor is associated with hyperglucagonemia, alpha cell hyperplasia, and islet cell tumor, *Pancreas* 38 (8) (2009) 941–946.
- [3] R. Yu, N.N. Nissen, D. Dhall, A.P. Heaney, Nesidioblastosis and hyperplasia of alpha cells, microglucagonoma, and nonfunctioning islet cell tumor of the pancreas: review of the literature, *Pancreas* 36 (4) (2008) 428–431.
- [4] R. Yu, Mahvash Disease: 10 Years After Discovery, *Pancreas* 47 (5) (2018) 511–515.
- [5] Dean ED, Li M, Prasad N, Wisniewski SN, Von Deylen A, Spaeth J, Maddison L, Botros A, Sedgeman LR, Bozadjieva N et al: Interrupted Glucagon Signaling Reveals Hepatic alpha Cell Axis and Role for L-Glutamine in alpha Cell Proliferation. *Cell Metab.* 2017, 25(6):1362–1373 (e1365).
- [6] J. Kim, H. Okamoto, Z. Huang, G. Anguiano, S. Chen, Q. Liu, K. Cavino, Y. Xin, E. Na, R. Hamid, et al., Amino acid transporter Slc38a5 controls glucagon receptor inhibition-induced pancreatic alpha cell hyperplasia in mice, *Cell Metab.* 25 (6) (2017) 1348–1361 (e1348).
- [7] E. Larger, N.J. Wewer Albrechtsen, L.H. Hansen, R.W. Gelling, J. Capeau, C.F. Deacon, O.D. Madsen, F. Yakushiji, P. De Meyts, J.J. Holst, et al., Pancreatic alpha-cell hyperplasia and hyperglucagonemia due to a glucagon receptor splice mutation, *Endocrinol. Diab. Metab. Case Rep.* 2016 (2016).
- [8] S.G. J Charrow, E. McCabe, P. Rinaldo, Tandem mass spectrometry in newborn screening. American College of Medical Genetics/American Society of Human Genetics Test and Technology Transfer Committee Working Group, *Genet. Med.* 2 (4) (2000) 267–269.
- [9] L.H. Zhao, Y. Yin, D. Yang, B. Liu, L. Hou, X. Wang, K. Pal, Y. Jiang, Y. Feng, X. Cai, et al., Differential Requirement of the Extracellular Domain in Activation of Class B G Protein-coupled Receptors, *J. Biol. Chem.* 291 (29) (2016) 15119–15130.
- [10] H. Zhang, A. Qiao, L. Yang, N. Van Eps, K.S. Frederiksen, D. Yang, A. Dai, X. Cai, H. Zhang, C. Yi, et al., Structure of the glucagon receptor in complex with a glucagon analogue, *Nature* 553 (7686) (2018) 106–110.
- [11] K.D. Galsgaard, M. Winther-Sorensen, C. Orskov, H. Kissow, S.S. Poulsen, H. Vilstrup, C. Prehn, J. Adamski, S.L. Jepsen, B. Hartmann, et al., Disruption of glucagon receptor signaling causes hyperaminoacidemia exposing a possible liver-alpha-cell axis, *Am. J. Physiol. Endocrinol. Metab.* 314 (1) (2018) E93–E103.
- [12] M. Ruitter, S.E. La Fleur, C. van Heijningen, J. van der Vliet, A. Kalsbeek, R.M. Buijs, The daily rhythm in plasma glucagon concentrations in the rat is modulated by the biological clock and by feeding behavior, *Diabetes* 52 (7) (2003) 1709–1715.
- [13] C.H. Gravholt, N. Moller, M.D. Jensen, J.S. Christiansen, O. Schmitz, Physiological levels of glucagon do not influence lipolysis in abdominal adipose tissue as assessed by microdialysis, *J. Clin. Endocrinol. Metab.* 86 (5) (2001) 2085–2089.
- [14] B. Sipes, J. Sperveslage, M. Anlauf, M. Hoffmeister, T. Henopp, S. Buch, J. Hampe, A. Weber, P. Hammel, A. Couvelard, et al., Glucagon cell hyperplasia and neoplasia with and without glucagon receptor mutations, *J. Clin. Endocrinol. Metab.* 100 (5) (2015) E783–E788.
- [15] R.W. Gelling, X.Q. Du, D.S. Dichmann, J. Romer, H. Huang, L. Cui, S. Obici, B. Tang, J.J. Holst, C. Fledelius, et al., Lower blood glucose, hyperglucagonemia, and pancreatic alpha cell hyperplasia in glucagon receptor knockout mice, *Proc. Natl. Acad. Sci. U. S. A.* 100 (3) (2003) 1438–1443.
- [16] H.P. Guan, X. Yang, K. Lu, S.P. Wang, J.M. Castro-Perez, S. Previs, M. Wright, V. Shah, K. Herath, D. Xie, et al., Glucagon receptor antagonism induces increased cholesterol absorption, *J. Lipid Res.* 56 (11) (2015) 2183–2195.
- [17] S. Han, T.E. Akiyama, S.F. Previs, K. Herath, T.P. Roddy, K.K. Jensen, H.P. Guan, B.A. Murphy, L.A. McNamara, X. Shen, et al., Effects of small interfering RNA-mediated hepatic glucagon receptor inhibition on lipid metabolism in db/db mice, *J. Lipid Res.* 54 (10) (2013) 2615–2622.